Catalysis Today 176 (2011) 424–428

Contents lists available at ScienceDirect

Catalysis Today

journal homepage: www.elsevier.com/locate/cattod

A study of the ammonia selectivity on $Pt/BaO/Al_2O_3$ model catalyst during the NO*x* storage and reduction process

N. Le Phuc, X. Courtois, F. Can*, S. Berland, S. Royer, P. Marecot, D. Duprez

Laboratoire de Catalyse en Chimie Organique, Université de Poitiers, UMR6503 CNRS, 40 Av. Recteur Pineau, Poitiers 86022, France

ARTICLE INFO

Article history:
Received 15 September 2010
Received in revised form 25 October 2010
Accepted 27 October 2010
Available online 27 November 2010

Keywords:
NO*x* storage
NO*x* reduction
Ammonia
Lean/rich cycles
Barium

ABSTRACT

The ammonia selectivity during the cycling NO*x* storage reduction process over a model $Pt/Ba/Al_2O_3$ catalyst was studied. Firstly, it was demonstrated that, whereas the presence of water or carbon dioxide in the gas mixture have a negative effect on the storage step, the effect of these components have different impacts on the NO*x* efficiency. Due to their involvement in the reverse water gas shift (RWGS) reaction, the absence of water in the gas mixture leads to a drop of the NO*x* removal whereas without CO_2, an increase of the NO*x* conversion is observed. It was also showed that the reducer (H_2) conversion during the short excursion in rich condition is directly correlated to the NH_3 emission. NH_3 is emitted since hydrogen is not fully converted, whatever the NO*x* conversion rate. The ammonia pathway is clearly demonstrated and it was claim that, when H_2 remains in the reaction mixture, the ammonia production rate is higher than the ammonia reaction with the remaining NO*x* in order to form N_2.

1. Introduction

As a result of environmental legislations on the CO_2 emission from automotive source, the development of diesel and lean-burn engines is in perpetual growth since several years. Due to the presence of excess of oxygen in the exhaust gas, abatement of NO*x* remains very difficult, and industrial or academic research groups are forced to propose new technological solutions. Thus, usually two main processes can be used to reduce NO*x* in excess of oxygen. The first one is the selective catalytic reduction (SCR) of NO*x*. Numerous reducers have been investigated in the literature, such as hydrocarbons [1–8], oxygenated compounds [5,6,9,10] and nitrogen containing compounds (ammonia, urea, etc.) [10–14]. The second possible solution is the use of the NO*x* storage reduction (NSR) catalyst [15], working in transient periods: during the lean condition, NO*x* are firstly oxidized and stored as nitrites or nitrates on a basic material, usually barium oxide. Periodically, the catalyst is regenerated: the stored NO*x* are reduced in N_2 during a short excursion in rich condition. Nevertheless the major drawback of this system is the deactivation of the catalyst, mainly due to sulfur poisoning [16,17], and the thermal aging [18,19]. It was also reported that ammonia emission can be formed during the short excursion under rich conditions, especially when hydrogen is used as reducer [20–25]. In the literature, it was suspected that the NH_3 production should be correlated to the barium loading [26], the temperature reaction [24,27,28] or the reducer concentration [29,30].

However, some points are still in opposition, and the objective of this work is to have a better understanding of the ammonia emission on $Pt/BaO/Al_2O_3$ model catalysts. Particularly, we have varied the catalytic test conditions in order to put in evidence the conditions of ammonia emission and its possible role in the NO*x* reduction. Moreover, we have studied the influence of CO_2 and H_2O on the NO*x* storage-reduction efficiency, as we have previously done for the NO*x* storage step [31].

2. Experimental part

2.1. Catalysts preparation

The reference catalyst contains 1 wt% Pt and 20 wt% BaO on alumina. Alumina powder (230 $m^2\,g^{-1}$) was suspended in a solution at 60 °C and pH 10, in order to ensure complete precipitation of the barium. The $Ba(NO_3)_2$ salt was then added under vigorous stirring, and the pH was maintained constant by ammonia addition. After 30 min, the solution was evaporated at 80 °C under air and the resulting powder was dried at 120 °C. After calcination at 700 °C, platinum (1 wt%) was impregnated using a $Pt(NH_3)_2(NO_2)_2$ aqueous solution. After drying, the catalyst was pre-treated at 700 °C for 4 h under N_2, in order to stabilize Pt and Ba before the final hydrothermal treatment at 700 °C for 4 h (10% O_2, 5% H_2O in N_2) [32]. The obtained catalysts are noted Pt/20Ba/Al and exhibits BET specific surface areas of 127 $m^2\,g^{-1}$.

* Corresponding author. Tel.: +33 05 49 45 39 97; fax: +33 05 49 45 34 99.
E-mail address: fabien.can@univ-poitiers.fr (F. Can).

0920-5861/$ – see front matter © 2010 Elsevier B.V. All rights reserved.
doi:10.1016/j.cattod.2010.10.080

2.2. Specific surface measurement

The BET surface areas were deduced from N_2 adsorption at −196 °C carried out with a Micromeritics apparatus. Prior to the measurement, the samples were treated at 250 °C under vacuum for 8 h in order to eliminate the adsorbed species.

2.3. XRD analysis

X-ray powder diffraction was performed at room temperature with a Bruker D5005 using a Kα Cu radiation (λ = 1.54056 Å). The powder was deposited on a silicon monocrystal sample holder. The crystalline phases were identified by comparison with the ICDD database files.

2.4. NOx storage capacity (NSC) measurement

Before each measurement, the catalyst (60 mg) was pretreated in situ for 30 min at 550 °C, under a 10% O_2, 10% H_2O, 10% CO_2 and N_2 mixture (total flow rate: 10 L h^{-1}), and then cooled down to the storage temperature under the same mixture. The sample was then submitted to a lean mixture as reported in Table 1, at 200 °C, 300 °C and 400 °C. The gas flow was introduced using mass-flow controllers, except for H_2O which was introduced using a saturator. Both NO and NO*x* concentrations (NO + NO_2) were followed by chemiluminescence. H_2O was removed prior to NO*x* analysis with a membrane dryer. Long time storage is not representative of the NSR catalyst working conditions, since the lean periods are commonly around 1 min. The NO*x* storage capacity was then estimated by the integration of the recorded profile for the first 60 s, which corresponds to the lean periods of the NSR test in cycling conditions. The contribution of the reactor volume is subtracted. With the conditions used in this test, 57.4 μmol NO*x* per gram of catalyst are injected in 60 s. In addition, the platinum oxidation activity was estimated as the NO_2/NO*x* ratio (%) at saturation (usually after about 900 s).

2.5. NOx conversion in cycling conditions

Before measurement, the catalyst (usually 60 mg if no other indications are given) was treated in situ at 450 °C under 3% H_2, 10% H_2O, 10% CO_2 and N_2 for 15 min. The sample was then cooled down to test temperatures (200, 300 and 400 °C) under the same mixture. The NO*x* conversion was studied in cycling condition by alternatively switching between lean and rich conditions using electro-valves. The lean and rich periods are 60 s and 3 s, respectively. The gas composition is described in Table 1. Hydrogen concentration in the rich pulse is usually 3%, but additional tests were performed with variable contents in hydrogen (1–9%).

NO and NO_2 were followed by chemiluminescence, N_2O by specific FTIR, H_2 by mass spectrometry. Before the analyzers, H_2O was removed in a condenser at 0 °C. For each studied temperature, the activity of the catalysts was followed until stabilization. After stabilization, the outlet water was condensed for 30 min in a dry condenser and then analyzed by two different HPLC for NH_4^+, NO_2^- and NO_3^-. NO_2^- and NO_3^- were added to the unconverted NO*x*. The N_2 selectivity is calculated assuming no other N-compounds than NO, NO_2, N_2O and NH_3. Some tests were also performed using a Multigas FTIR detector (MKS 2030) without water trap system and same results were then obtained.

3. Results and discussion

The X ray diffractogramms obtained with reference Pt/20Ba/Al before and after the platinum impregnation step were previously studied in [31,33]. It was demonstrated that the main crystallized phases detected are $BaCO_3$ and $BaAl_2O_4$. Some phase transformation occurred during the platinum addition. The XRD pattern of the 20Ba/Al support powder exhibits significantly more intense $BaCO_3$ and $BaAl_2O_4$ diffraction peaks than for the platinum supported Pt/20Ba/Al catalyst. It can be attributed to barium leaching from the support during the platinum impregnation step [34,35].

3.1. Effect of water and carbon dioxide on the NOx storage-reduction (NSR) process

During the first step of NO*x* storage reduction (NSR) process, NO*x* are stored on basic sites of the support. In order to understand the role of water and carbon dioxide on the whole NSR process, their influences were firstly investigated on the NO*x* storage step. The effect of water is studied in the presence of CO_2 and the effect of CO_2 is studied in the presence of H_2O.

3.1.1. NOx storage measurements

Fig. 1 displays the effect of water and carbon dioxide on the NO*x* storage rate for 60 s for the Pt/20Ba/Al model catalyst. The NO oxidization activity is assessed using the NO_2/NO*x* ratio measured after saturation (commonly after 900 s). Firstly, with H_2O and CO_2 in the gas mixture, it appears that the NO*x* storage capacity increases versus temperature, from 57% at 200 °C until 83% at 400 °C. Then, whatever the temperature test, the inlet NO*x* are not totally stored in 60 s. With the complete gas mixture, results reported in Fig. 1 show that NO_2/NO*x* ratio is about 9% at 200 °C and increases continually with temperature to reach 42% at 400 °C.

In order to study the influence of water, some tests were performed without H_2O in the reaction mixture. Tests without water lead to significant enhancements of the NO*x* storage capacities, from 73% at 200 °C, to a total stored NO*x* at 400 °C (98%, Fig. 1). As previously observed [31], this can be attributed to the inhibiting effect of water on the NO to NO_2 oxidation rate. Indeed, the NO_2/NO*x* ratios after storage saturation with water in the feed stream are 9%, 21% and 42% at 200, 300 and 400 °C, respectively. When H_2O is removed, they reach 18%, 30% and 48%, respectively.

When CO_2 is removed from the feed gas, the NO*x* storage capacities also increase. Near all the introduced NO*x* are trapped at 300 and 400 °C (Fig. 1). In another words, the inhibiting effect of CO_2 is stronger compared with the H_2O inhibiting effect. In opposition with H_2O, CO_2 has no influence on the NO to NO_2 oxidation rate since the NO_2/NO*x* ratios at saturation remain unchanged when CO_2 is removed from the reaction mixture. The inhibiting effect of CO_2 on the NO*x* storage was attributed to the competition between nitrates and carbonates formation on the storage sites [31].

3.1.2. NOx storage-reduction (NSR) efficiency

Results on the influence of water and carbon dioxide on the NO*x* storage-reduction efficiency are reported in Fig. 2. The H_2 concentration in the rich pulse is 3% (duration: 3 s).

First, note that N_2O was never significantly observed during these tests in cycling condition, whatever the temperature test. This point is consistent with the study of Abdulhamid et al. [24] who claims that N_2O is mainly obtained with CO as reducer. Besides, whatever the tested temperatures, comparison of Figs. 1 and 2 shows that the NO*x* reduction efficiency is always lower than the NO*x* storage rate, showing that the limiting step of this process is the reduction phase. This observation is confirmed by the fact that the introduced hydrogen is not fully converted, whatever the temperature. Using the complete mixture, including H_2O and CO_2, the maximum NO*x* conversion is obtained at 400 °C and reaches only 45%. In addition, the ammonia selectivity is rather high. It reaches around 20% at 200 °C and 300 °C and 33% at 400 °C.

In opposition with the storage tests, NO*x* storage/reduction tests in absence of water, leads to a deterioration in the reduction rate,

Table 1
Rich and lean gas compositions used for the NO*x* conversion test (60 s lean/3 s rich). Total flow rate: 10 L h^{-1}.

Gas	NO	H_2	O_2	CO_2	H_2O	N_2
Rich	–	1–9%	–	10%	10%	Balance
Lean	500 ppm	–	10%	10%	10%	Balance

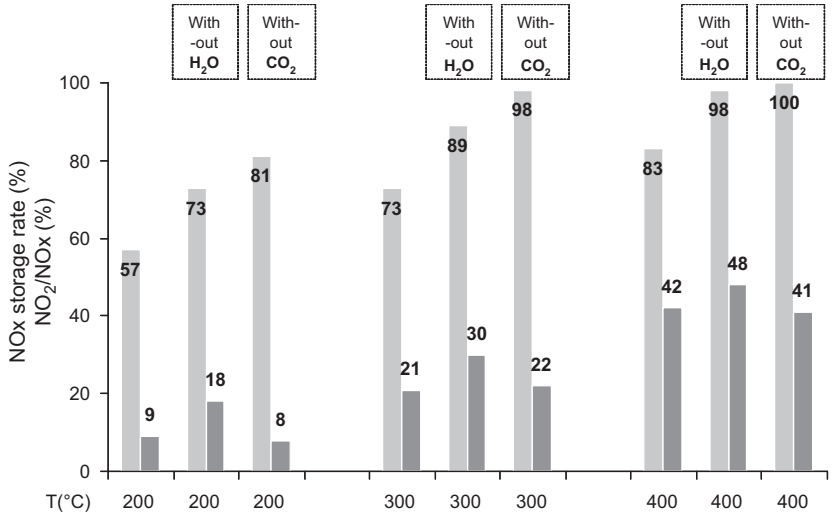

Fig. 1. NO*x* storage rate (■) and NO_2/NO*x* ratio (■) versus temperature toward Pt/20Ba/Al model catalyst.

especially at 200 °C. This can be attributed to the reverse water gas shift reaction (RWGS, $CO_2 + H_2 \leftrightarrows CO + H_2O$) which is favored in absence of water, and lead to the production of CO, confirmed by the measurement of 350 ppm (detected at the outlet with a Multigas FTIR analyzer, MKS 2030). Since H_2 is reported to be more active than CO for NO*x* reduction at low temperature [15], it explains results reported in Fig. 2. Besides, note that, while NO*x* conversion is lower without H_2O, the H_2 conversion increases (Fig. 2), showing that the reducer also react with CO_2, according to the RWGS reaction. Moreover, the reverse water gas shift reaction can also explain the higher ammonia selectivity in absence of water observed at 300 and 400 °C. Indeed, Lesage et al. [36,37] have proposed that the NH_3 formation come from the isocyanate hydrolysis ($2\,NCO + 3H_2O \leftrightarrows 2NH_3 + 2CO_2 + 1/2\,O_2$) when CO is present during the rich periods. Besides, even if H_2O is not present in the gas mixture, it is not the limiting reactant for the isocyanate hydrolysis reaction since the converted hydrogen is mainly oxidized in H_2O.

It was previously reported in Fig. 1 that CO_2 inhibits the NO*x* storage, with a drop around 20–30%. During the NO*x* storage/reduction test in cycling condition, CO_2 leads to a higher loss between 35% and 45%. Thus, CO_2 also inhibits the reduction step. It can be attributed to a higher NO*x* desorption rate during the rich pulses when CO_2 is added in the reaction mixture [38], leading to higher NO*x* slip. Furthermore, with CO_2 in the feed stream, the reverse water gas shift reaction ($CO_2 + H_2 \leftrightarrows CO + H_2O$) is favored. H_2 is partially converted into CO which is less active than hydrogen for the NO*x* reduction [15]. Another interesting point is the relatively low ammonia selectivity when CO_2 is removed from the feed stream. In fact, without CO_2, the CO formation (via the RWGS reaction) is not possible. As a consequence, formation of isocyanate, which is considered as ammonia precursor [36,37], is unexpected.

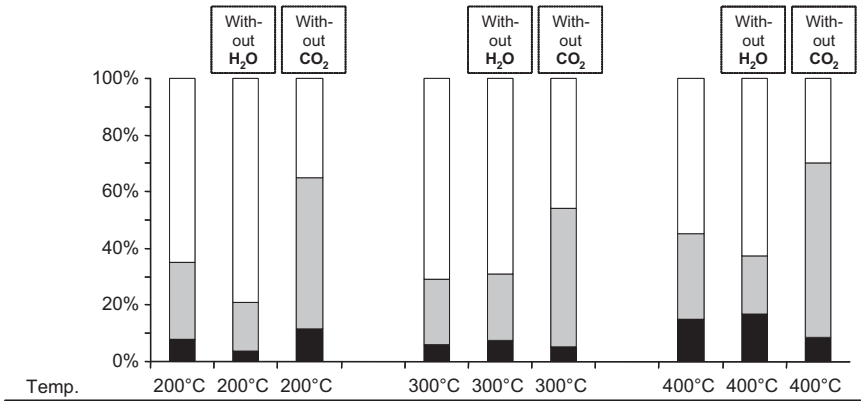

Temp.	200°C	200°C	200°C	300°C	300°C	300°C	400°C	400°C	400°C
H_2 conv.	73%	86%	86%	70%	81%	81%	90%	93%	93%
N_2 selec.	78%	83%	82%	79%	76%	90%	67%	59%	88%
NH_3 selec.	22%	17%	18%	21%	24%	10%	33%	41%	12%
NOx conv.	35%	21%	65%	29%	31%	54%	45%	41%	70%

Fig. 2. Pt/20Ba/Al catalyst (60 mg): NO*x* storage/reduction efficiency test at 200, 300 and 400 °C with 3% H_2 in the rich pulses. NO*x* conversion (%) into N_2 (■) and into NH_3 (■) and related data. Influence of CO_2 and H_2O.

Table 2
Effect of H_2 concentration on the NSR efficiency at 400 °C with 60 mg of the Pt/20Ba/Al catalyst.

H_2 inlet in the rich pulses (%)	1	1.5	2	3	4	5	6	9
H_2 conv. (%)	99	95	88	85	69	61	63	55
S_{N_2} (%)	87	80	67	67	60	57	57	53
S_{NH_3} (%)	13	20	33	33	40	43	43	47
NO*x* conv. (%)	37	41	44	45	44	45	48	49

However, NH_3 is detected at a lower level even if there is no carbon source in the used reaction mixture. It induces that the isocyanate hydrolysis is not the only way to obtain ammonia.

To conclude, water and carbon dioxide have an important impact in the RWGS reaction. In absence of water in the gas mixture, the production of CO is enhanced, leading to a drop of the NO*x* reduction and an increase of the ammonia production at high temperature. These results are explained by the fact that CO has been advanced as a precursor of intermediates isocyanates species, involved in the ammonia reaction pathway. A similar trend is observed with CO_2. In fact in absence of carbon dioxide, the CO formation is not possible, and the ammonia yield consistently decreases.

3.2. Effect of hydrogen concentration on the NSR efficiency

Effect of H_2 concentration (from 1% up to 9%) on the NSR efficiency at 400 °C is reported in Table 2. Results were obtained with both H_2O and CO_2 in the feed stream.

First, with 60 mg of catalyst, it appears from results display in Table 2, that the increase of the H_2 concentration leads to only a small increase of the NO*x* conversion, from 37% with 1% H_2 to 49% with 9% H_2. In parallel, a significant increase of the NH_3 selectivity is measured with the increase of the H_2 conversion, showing that the higher the hydrogen consumed, the lower the NH_3 produced. However, whatever the H_2 concentration in the inlet gas, hydrogen was never fully converted. In order to study the catalyst behavior at higher hydrogen consumption, some supplementary tests were performed with higher catalyst weight. Results are reported in Table 3 and Fig. 3.

The evolution of NO*x* conversion as well as the nitrogen selectivity versus the amount of hydrogen in the rich pulse are presented in Fig. 3. It appears that the increases of the hydrogen concentration lead to a significant enhancement the NO*x* conversion, especially when H_2 concentration varies between 1% and 2.5% in the rich pulses. In a same time, on this hydrogen range, no ammonia emission is observed, and H_2 is fully converted (Table 3).

For higher H_2 concentration (3–6%), NO*x* conversion varies only between 83% and 87%. In parallel, NH_3 selectivity strongly increases from 17% to 42%, and hydrogen is then not fully converted.

To conclude, the fact that NO*x* conversion increases, whereas H_2 is fully converted and that no ammonia emission was observed, suggests a NO*x* reduction by NH_3 as reducer. This assumption was examined assuming three parts in the catalytic bed: 60 mg, 100 mg and 140 mg. Catalytic tests were performed with 2%, 3% and 6% of hydrogen in the rich pulses and only results with 2% of H_2 at 400 °C are presented in Table 4. It was observed that, when catalyst weight increases, H_2 conversion increases. In parallel, NH_3 selectivity decreases until no ammonia emission was detected when H_2 is fully converted. In the same time NO*x* conversion is enhanced.

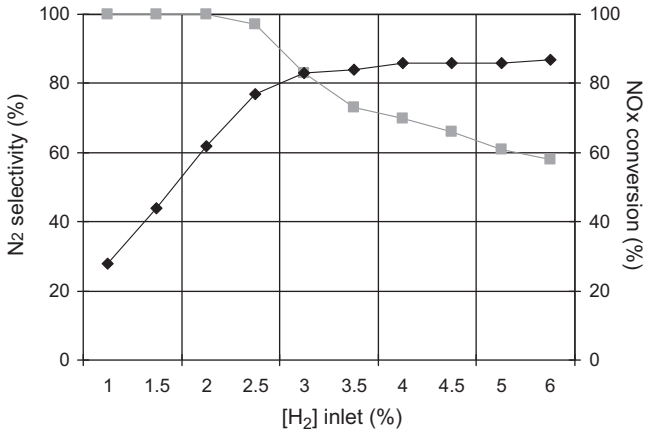

Fig. 3. Nitrogen selectivity (■) and NO*x* conversion (♦) versus the amount of hydrogen in the rich pulse with 140 mg of Pt/20Ba/Al catalyst at 400°C.

Table 4
Effect of the Pt/20Ba/Al catalyst weight at 400 °C on the NSR efficiency for 2%, 3% and 6% of hydrogen in the rich pulse.

H_2 inlet	2%		
Catalyst weight (mg)	60	100	140
H_2 conv. (%)	88	99	100
S_{N_2} (%)	67	85	100
S_{NH_3} (%)	33	15	0
NO*x* conv. (%)	44	52	62

4. Discussion

From the results presented below, ammonia intermediate pathway was clearly demonstrated for the reduction of the stored NO*x* with H_2. It appears that, when hydrogen is missing in the rich pulses, that is fully converted, the ammonia selectivity tends to be nil because the produced NH_3 can react with the remaining stored NO*x*. In opposition, if some hydrogen remains, the ammonia selectivity increases with the amount of excessive hydrogen. It induces that NO*x* reduction with H_2 into ammonia is faster than the NO*x* selective catalytic reduction with ammonia. This hypothesis is in accordance with the proposition of Lindholm et al. [30]. They have observed that during a long time rich period of several minutes, ammonia is not emitted at the beginning of the rich phase. They have suggested that the in situ produced ammonia firstly react with the stored NO*x*. According to Cumaranatunge et al. [30], NH_3 is as

Table 3
Effect of H_2 concentration on the NSR efficiency at 400 °C with 140 mg of the Pt/20Ba/Al catalyst.

H_2 inlet in the rich pulses (%)	1	1.5	2	2.5	3	3.5	4	4.5	5	6
H_2 conv. (%)	100	100	100	100	99	97	90	88	84	79
S_{N_2} (%)	100	100	100	97	83	73	70	66	61	58
S_{NH_3} (%)	0	0	0	3	17	27	30	34	39	42
NO*x* conv. (%)	28	44	62	77	83	84	86	86	86	87

efficient as H_2 for the NO*x* reduction on Pt/Ba/Al_2O_3, which explain the delay for the NH_3 emission.

In order to check the catalyst activity for the NO*x* SCR with ammonia, additional tests were performed. In the literature, fast and slow NH_3-SCR reaction can be considered, respectively in oxidizing or in stoichiometric condition. The last condition seems more auspicious to the NSR results presented below (i.e, without oxygen in the rich pulse). Thus, the slow SCR corresponds to stoichiometric mixture according the reaction $4NH_3 + 6NO \rightarrow 5N_2 + 6H_2O$. This condition was tested between 150 °C and 450 °C using a 5 °C min^{-1} heating rate with simplified reaction mixtures: 333 ppm NH_3 and 500 ppm NO balanced in N_2 (m_{cata}: 60 mg; total flow rate: 12 L h^{-1}, results not shown). It was evidenced that NO and NH_3 conversion start near 180 °C and they are fully converted in N_2 for temperature higher than 220 °C. N_2O is observed only near 200 °C, with a maximum yield of 20%.

Thus, without oxygen in the feed stream, the NO SCR into N_2 only is obtained from 220 °C with the Pt/Ba/Al catalyst and using ammonia as reducer (light-off mode). This result confirms the previous hypothesis about the reaction of ammonia produced in situ during the rich pulses and the stored NO*x* to form N_2.

5. Conclusion

Pt/20Ba/Al catalyst was used as a reference material for the study of the NO*x* storage-reduction process. Effect of water and carbon dioxide toward the NO*x* efficiency was measured at 200 °C, 300 °C and 400 °C, and compared with the NO*x* storage properties of the sample. Finally, H_2O and CO_2 both inhibit the NO*x* storage, because of NO oxidation inhibition and carbonate/nitrate competition, respectively. Concerning the reduction step, water induces a positive effect by limiting the hydrogen transformation into CO via the reverse WGS. On the contrary, CO_2 favors the fast NO*x* desorption during the rich pulses promotes the hydrogen transformation into CO which is less efficient for the NO*x* reduction and leads to higher ammonia formation rate via the isocyanate pathway.

A special attention was then carried out on the ammonia emission of the reduction step. It was clearly demonstrated that the N_2 selectivity strongly depends on the hydrogen conversion introduced during the rich pulses. NH_3 is emitted since hydrogen is not fully converted, whatever the NO*x* conversion rate. The ammonia selectivity increases with the hydrogen excess. Then, the ammonia pathway is clearly put in evidence. In addition, when H_2 remains in the reaction mixture, the ammonia production rate is higher than the ammonia reaction with NO*x* in order to form N_2.

References

[1] M. Konsolakis, I.V. Yentekakis, J. Catal. 198 (2001) 142.
[2] J. Shibata, K.-I. Shimizu, A. Satsuma, T. Hattori, Appl. Catal. B 37 (2002) 197.
[3] E.F. Iliopoulou, A.P. Evdou, A.A. Lemonidou, I.A. Vasalos, Appl. Catal. A 274 (2004) 179.
[4] L.F. Cordoba, W.M.H. Sachtler, C.M. de Correa, Appl. Catal. B 56 (2005) 269.
[5] T. Maunula, J. Ahola, H. Hamada, Appl. Catal. B 26 (2000) 173.
[6] E. Joubert, X. Courtois, P. Marecot, D. Duprez, Appl. Catal. B 64 (2006) 103.
[7] P. Denton, A. Giroir-Fendler, H. Praliaud, M. Primet, J. Catal. 189 (2000) 410.
[8] F. Figueras, J.L. Flores, G. Delahay, A. Giroir-Fendler, A. Bouranea, J.-M. Clacens, A. Desmartin-Chomel, C. Lehaut-Burnouf, J. Catal. 232 (2005) 27.
[9] D. Tran, C.L. Aardahl, K.G. Rappe, P.W. Park, C.L. Boyer, Appl. Catal. B 48 (2004) 155.
[10] K.O. Haj, S. Ziyade, M. Ziyad, F. Garin, Appl. Catal. B 37 (2002) 49.
[11] N.W. Cant, A.D. Cowan, I.O.Y. Liu, A. Satsuma, Catal. Today 5 (1999) 473.
[12] N.W. Cant, I.O.Y. Liu, Catal. Today 63 (2000) 133.
[13] V. Zuzaniuk, F.C. Meunier, J.R.H. Ross, J. Catal. 202 (2001) 340.
[14] I.O.Y. Liu, N.W. Cant, J. Catal. 230 (2005) 123.
[15] W.S. Epling, L.E. Campbell, A. Yezeerets, N.W. Currier, J.E. Parks II, Catal. Rev. 46 (2004) 163.
[16] C. Sedlmair, K. Seshan, A. Jentys, J.A. Lercher, Catal. Today 75 (2002) 413.
[17] E.C. Corbos, X. Courtois, N. Bion, P. Marecot, D. Duprez, Appl. Catal. B 80 (2008) 62.
[18] D. Uy, A.E. O'Neill, J. Li, W.L.H. Watkins, Top. Catal. 95 (2004) 191.
[19] M. Casapu, J.D. Grunwaldt, M. Maciejewski, M. Wittrock, U. Göbel, A. Baiker, App. Catal. B 63 (2006) 232.
[20] R.D. Clayton, M.P. Harold, V. Balakotaiah, Appl. Catal. B 84 (2008) 616–630.
[21] L. Lietti, I. Nova, P. Forzatti, J. Catal. 257 (2008) 270–282.
[22] I. Nova, L. Lietti, L. Castoldi, E. Tronconi, P. Forzatti, J. Catal. 239 (2006) 244–254.
[23] Z. Liu, J.A. Anderson, J. Catal. 224 (2004) 18–27.
[24] H. Abdulhamid, E. Fridell, M. Skoglundh, Top. Catal. 30/31 (2004) 161–168.
[25] W.P. Partrige, J.-S. Choi, Catal. Appl. B. 91 (2009) 144.
[26] L. Castoldi, I. Nova, L. Lietti, P. Forzatti, Catal. Today 96 (2004) 43–52.
[27] I. Nova, L. Castoldi, L. Lietti, E. Tronconi, P. Forzatti, Top. Catal. 42/43 (2007) 21–25.
[28] A. Lindholm, N.W. Currier, A. Yezerets, L. Olsson, Top. Catal. 42–43 (2007) 83–89.
[29] J.A. Pihl, J.E. Parks II, C.S. Daw, T.W. Root SAE Technical Paper, 01-3441, 2006.
[30] A. Lindholm, N.W. Currier, E. Fridell, A. Yezerets, L. Olsson, Appl. Catal. B 75 (2007) 78–87.
[31] E.C. Corbos, X. Courtois, N. Bion, P. Marécot, D. Duprez, Appl. Catal. B 76 (2007) 357–367.
[32] E.C. Corbos, X. Courtois, F. Can, P. Marécot, D. Duprez, Appl. Catal. B 84 (2008) 514–523.
[33] P.N. Lê, E.C. Corbos, X. Courtois, F. Can, S. Royer, P. Marecot, D. Duprez, Top. Catal. 52 (2009) 1771–1775.
[34] G.W. Graham, H.W. Jen, H.W. Theis, R.W. McCabe, Catal. Lett. 93 (2004) 3–6.
[35] D.H. Kim, Y.H. Chin, I.H. Kwak, J. Szanyi, C.H.F. Peden, Catal. Lett. 105 (2005) 259–268.
[36] T. Lesage, C. Verrier, P. Bazin, J. Saussey, M. Daturi, Phys. Chem. Phys. Chem. Chem. Phys. 5 (2003) 4435–4440.
[37] T. Lesage, C. Verrier, P. Bazin, J. Saussey, S. Malo, C. Hedouin, G. Blanchard, M. Daturi, Top. Catal. 30–31 (2004) 31–36.
[38] S. Balcon, C. Potvin, L. Salin, J.F. Tempère, G. Djega-Mariadassou, Catal. Lett. 60 (1999) 39–43.